FOR REFERENCE

NOT TO BE TAKEN FROM THIS ROOM

NACA

RESEARCH MEMORANDUM

VIBRATION SURVEY OF BLADES IN 10-STAGE AXIAL-FLOW COMPRESSOR

III - PRELIMINARY ENGINE INVESTIGATION

By André J. Meyer, Jr. and Howard F. Calvert

Lewis Flight Propulsion Laboratory
Cleveland, Ohio

NATIONAL ADVISORY COMMITTEE
FOR AERONAUTICS

WASHINGTON
January 31, 1949

3 1176 01435 5631

RESTRICTED

NATIONAL ADVISORY COMMITTEE FOR AERONAUTICS

RESEARCH MEMORANDUM

VIBRATION SURVEY OF BLADES IN 10-STAGE AXIAL-FLOW COMPRESSOR

III - PRELIMINARY ENGINE INVESTIGATION

By André J. Meyer, Jr. and Howard F. Calvert

SUMMARY

Strain gages were used to measure blade vibrations possibly
causing failure in the 10-stage compressor of a jet-propulsion
engine. The seventh and tenth stages were of great concern as a
result of failures experienced by the manufacturer. Strain-gage
records were obtained from all stages during acceleration, decelera-
tion, and constant speed runs. Curves are presented showing the
maximum allowable vibratory stress for a given speed, the change of
the damping coefficient with the mounting of a strain gage at the
base of the blade, the effect of rotor speed on blade natural fre-
quency, and the effect of the order of first bending-mode vibra-
tion on stress. It was found that for all stages the lower the
order of vibration the higher the stress but no destructive vibra-
tions were detected.

INTRODUCTION

Blade failures in an early experimental 10-stage axial-flow
compressor of a jet-propulsion engine, presumably caused by vibration,
have been reported by the manufacturer. The failures are believed
to have originated in the seventh and tenth stages at high engine
speed and high pressure ratio. A series of vibration surveys is
being conducted at the NACA Lewis laboratory to determine the
cause of these failures and to devise a means of eliminating them.

Little published information is available on experimental
measurements of the factors that cause blade vibration; the vibration
characteristics were therefore investigated in a jet engine under
actual operating conditions. Prior to the dynamic investigation
(reference 1), the natural frequencies and node shapes of various
modes of blade vibrations were determined and with these data,
critical-speed diagrams were plotted for each of the 10 stages of
the compressor rotor (reference 2).

The preliminary dynamic investigation consisted in instrumenting the rotor and in measuring blade vibrations while the compressor was driven by an electric drive motor. The results obtained are presented in reference 1. The data are incomplete for analytical use because a drive motor with sufficient power to operate the compressor at rated speed for sea-level conditions was unavailable at the time.

The same compressor was then reinstrummented and assembled within a complete jet engine in order to continue the vibration surveys to maximum rated speed and power. Curves are included to show the effects of both engine speed and the orders of excitations on vibratory stresses and frequencies. Statically determined damping coefficients and relations between vibration amplitude and vibrational stresses or loads are also reported.

APPARATUS AND PROCEDURE

Before instrumentation, the rotor used in reference 1 was returned to the manufacturer for complete reblading because the original set of blades had been twisted by the manufacturer in an effort to improve the compressor efficiency and therefore may have had different vibration characteristics from those engines that failed.

The compressor rotor was reinstrumented with the types of strain gage, lead wire, slip-ring assembly, and electric circuit described and illustrated in reference 1. The only significant changes in the gage installation were: (1) All gages were mounted on the blades in such a position as to detect the first bending-mode vibration, because no torsional- or other significant bending-mode vibrations were observed in the first dynamic-vibration investigation; and (2) a transparent, polymerizing, coil-impregnating material was substituted for the ceramic cement previously used to embed the lead wires in the drilled rotor holes. In the initial dynamic investigation (reference 1), data from the last five stages were inconclusive because many lead wires were torn loose by centrifugal force before completion of the investigation.

After the strain gages were installed, frequency and damping measurements were made to evaluate the effect of the gage and its cement on vibration characteristics. The frequencies were determined by the method reported and illustrated in reference 2 and damping values were calculated from vibration die-away curves produced by plucking the blade and recording the vibration with a capacitance pickup.

The rebladed compressor was then assembled in a late production jet engine (fig. 1) and mounted on a sea-level-type test stand. The inlet guide vanes furnished with this engine transferred part of the compression load from the rear stages, in which failures had originated, to the front stages. A variable-area clamshell tail cone was substituted for the original jet assembly in an attempt to make it possible to vary the back pressure and consequently the pressure ratio of the compressor.

The rotor speed was varied until blade vibrations were indicated by the strain-gage signals, at which time the speed was held constant while photographic records were taken. The engine was accelerated and decelerated at 400 rps over the entire speed range, permitting the vibrations to build up to maximums, while continuous records were being taken. The amount of vibratory stress indicated was determined by comparing signal heights recorded with the heights of signals produced by a calibration instrument using similar strain gages. The vibratory-stress signals were corrected for the frequency response of the recording equipment.

Loads were applied at the tips of the instrumented blades and corresponding tip deflections and bending stresses were measured. Thus the observed vibratory stresses were correlated with the tip amplitudes of the blades.

DISCUSSION AND RESULTS

The critical-speed diagrams plotted in reference 2 indicated that the blade failures possibly could have resulted from resonant vibration caused by a fourth-order excitation (four force impulses per revolution of the rotor) in the seventh stage or by a sixth-order excitation in the tenth stage. Exciting forces are generally thought to be caused either by regularly spaced discontinuities in the air stream or by load impulses transmitted mechanically from various engine components. Sources of fourth- and sixth-order excitations of either type are not readily apparent in the engine. Four bearing-support arms are in the front of the engine, but it is doubtful that their effect would be prominent in the seventh stage after the air has churned through the six preceding stages. The first vibration survey conducted on the compressor (reference 1) definitely determined, however, the presence of fourth- and sixth-order impulses, as well as many others in all instrumented stages. The gravity of these fourth- and sixth-order impulses could

not be evaluated in the seventh and tenth stages during the prelim-
inary dynamic investigation because the resonant condition required
speeds higher than those obtainable.

The rotor used in this investigation came from one of the first
experimental jet units and apparently a tolerance change or a change
due to the reblading caused the natural frequencies of the new blades
to be higher than those of the original blades. It was found that
the average of the natural frequencies of the new blades was 9.8 per-
cent higher than that previously determined in reference 2. This
increase in natural frequency and a 4.7-percent average increase in
frequency induced by the stiffening effect of the strain-gage instal-
lation made it impossible to reach a fourth- and sixth-order resonant
condition in the seventh and tenth stages, respectively, without
dangerously overspeeding the engine. Artificial reduction of the
natural frequencies may permit attainment of these resonances.

A critical-speed diagram (measured vibratory frequency plotted
against rotor speed) showing the orders of vibration encountered is
presented in figure 2. Excitation forces from the third to the
seventeenth order apparently are present within the compressor and
vibrations caused by the orders are exact multiples of rotor speed.
A comparison of calculated and measured effect of centrifugal force
on blade natural frequency similar to figure 6 of reference 1 is
shown in figure 3. Order of excitation is plotted against measured
vibratory stress in figure 4. For all stages, the lower the order
of vibration the higher the stress and all stages show the same
general slope. All the vibratory stresses plotted are produced by
first bending-mode vibrations of the cantilever compressor blades.
Each stage has an exception to the general trend; some orders are
predominant, others are absent. For example, in the tenth stage
(fig. 4(c)), the seventeenth order results in the highest stress
whereas the eighth, ninth, and twelfth lie below the trend. The
source of the high stress at the seventeenth order as well as the
source of the other exceptions was undetermined.

The records taken during engine acceleration and deceleration
gave a complete account of all vibrations present throughout the
speed range. No obviously serious vibration was present during
either acceleration or deceleration. The vibratory stresses and
consequently the vibration amplitudes for the acceleration and
deceleration runs were very nearly equal to those for conditions in
which the speed was set and held at the peak-resonance point.

The vibrational stresses thus far observed are relatively low
and would not in themselves result in blade failure. The highest
vibratory stress recorded was ±8250 pounds per square inch, which

906

occurred in the third stage and was excited by a fourth-order source.
The maximum allowable vibratory stress over the range of rotor speeds
is shown in figure 5. Allowable stresses of the intervening stages
lie between the curves of the two extreme stages plotted. Data for
figure 5 were obtained from calculations of mean working stress
(centrifugal stress plus bending stress) and the relation given in
reference 3 between mean stress and total allowable stress for the
blade material. Vibratory stresses of approximately 35,000 pounds
per square inch are necessary to cause failure of the seventh- and
tenth-stage blades according to figure 5.

It was suspected that part of the cause for the low measured
vibratory stresses might be the additional damping introduced by
the presence of the strain gage. The damping values were measured
at static conditions for blades with and without gages. In the last
five stages, the vibratory stresses might have been reduced by gage
installation, as indicated by figure 6; the information is inconclu-
sive, however, because the effect of rotational forces on damping
properties is unknown. The inlet guide vanes used also may have
lowered the vibrational stresses as well as the compression load,
consequently reducing the bending stresses in the rear stages of the
compressor. The results of static tests performed to correlate the
vibratory-stress magnitudes with the tip amplitudes and with loads
of the blades are shown for the seventh and tenth stages in figure 7.
Extrapolation of this information indicates that vibrations with tip
amplitudes of ±0.055 and ±0.084 inch must be attained to cause
failure of seventh- and tenth-stage blades, respectively.

When the compressor was driven by an electric drive motor,
throttling the exhaust and thus raising the pressure ratio had a
pronounced effect on the vibration amplitude (reference 1). The
engine used in succeeding investigations was therefore equipped with
a clamshell arrangement providing a variable-area tail cone. A
resonant condition of engine speed was set, as in the drive-motor
experiments, and the tail-cone area was varied over the maximum
range permitted by allowable turbine temperatures. No change in
vibration amplitude was noticed, however, probably because the varia-
tion in pressure ratio was small and because the compressor inherently
operated near the pressure ratio that is the maximum obtainable for
any particular speed of the engine.

SUMMARY OF RESULTS

From an investigation of vibratory stresses in a 10-stage axial-
flow compressor conducted by means of strain gages mounted on blades
of each stage, the following results were obtained:

· 1. First bending-mode vibrations were detected at each exact multiple of rotor speed from 3 to 17.

2. Fourth and sixth orders of first bending-mode vibration in the seventh and tenth stages, respectively, could not be measured without serious overspeeding of the compressor.

3. No destructive vibrations were observed in the rebladed compressor throughout its normal operating range as investigated in the complete engine.

4. For all stages, it was found that the higher the order of vibration the lower the stress. An exception to the trend was discovered in each stage.

Lewis Flight Propulsion Laboratory,
        National Advisory Committee for Aeronautics,
                Cleveland, Ohio.

REFERENCES

1. Meyer, André J., Jr., and Calvert, Howard F.: Vibration Survey of Blades in 10-Stage Axial-Flow Compressor. II - Dynamic Investigation. NACA RM No. E8J22a, 1949.

2. Meyer, André J., Jr., and Calvert, Howard F.: Vibration Survey of Blades in 10-Stage Axial-Flow Compressor. I - Static Investigation. NACA RM No. E8J22, 1949.

3. Noll, G. C., and Lipson, C.: Allowable Working Stresses. Proc. Soc. Exp. Stress Analysis, vol. III, no. 2, 1946, pp. 89-101.
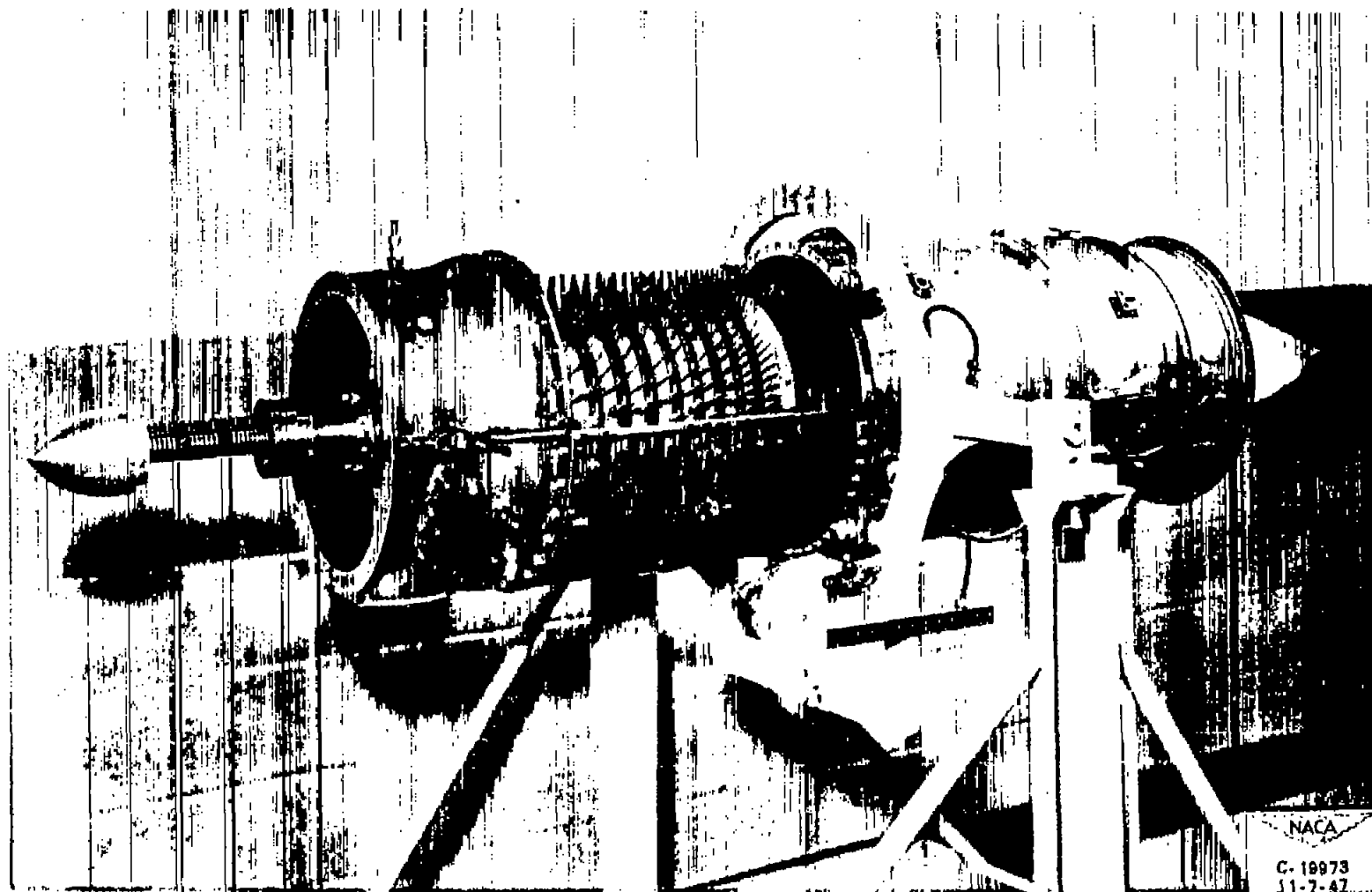
Figure 1. - Ten-stage axial-flow compressor installed in jet engine.

906

⊦
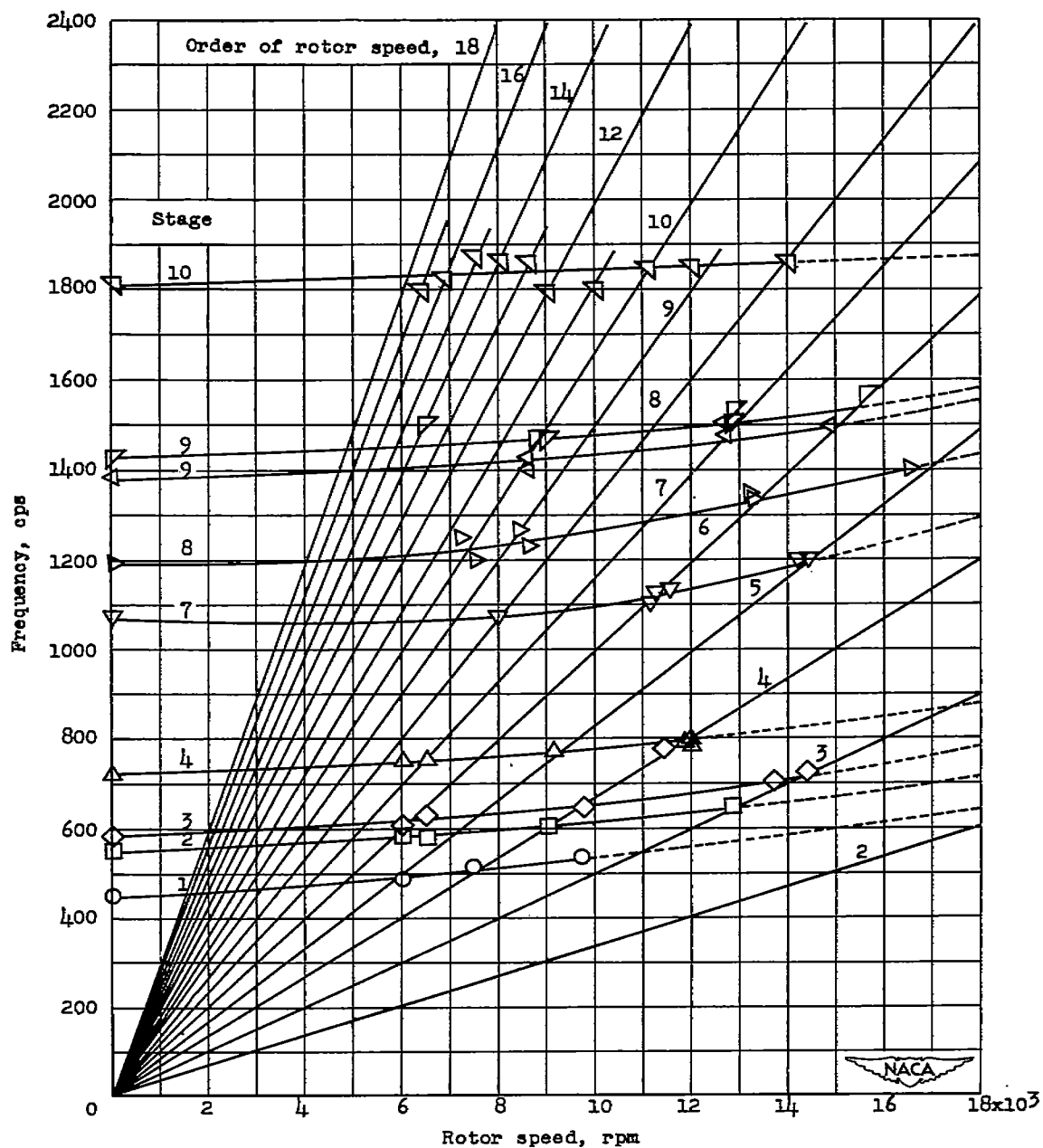
Figure 2. - Critical-speed diagram showing measured first bending-mode frequencies
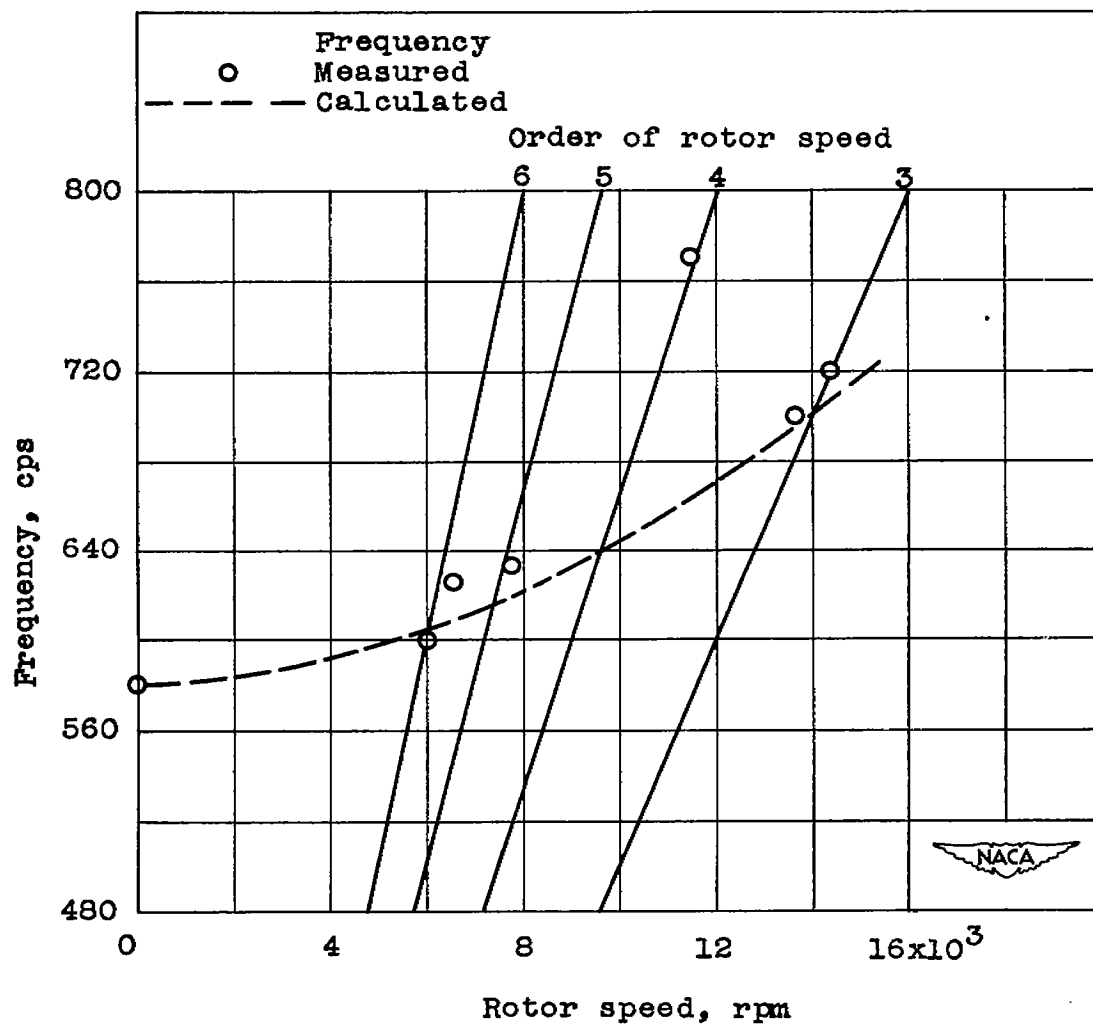for various stages.
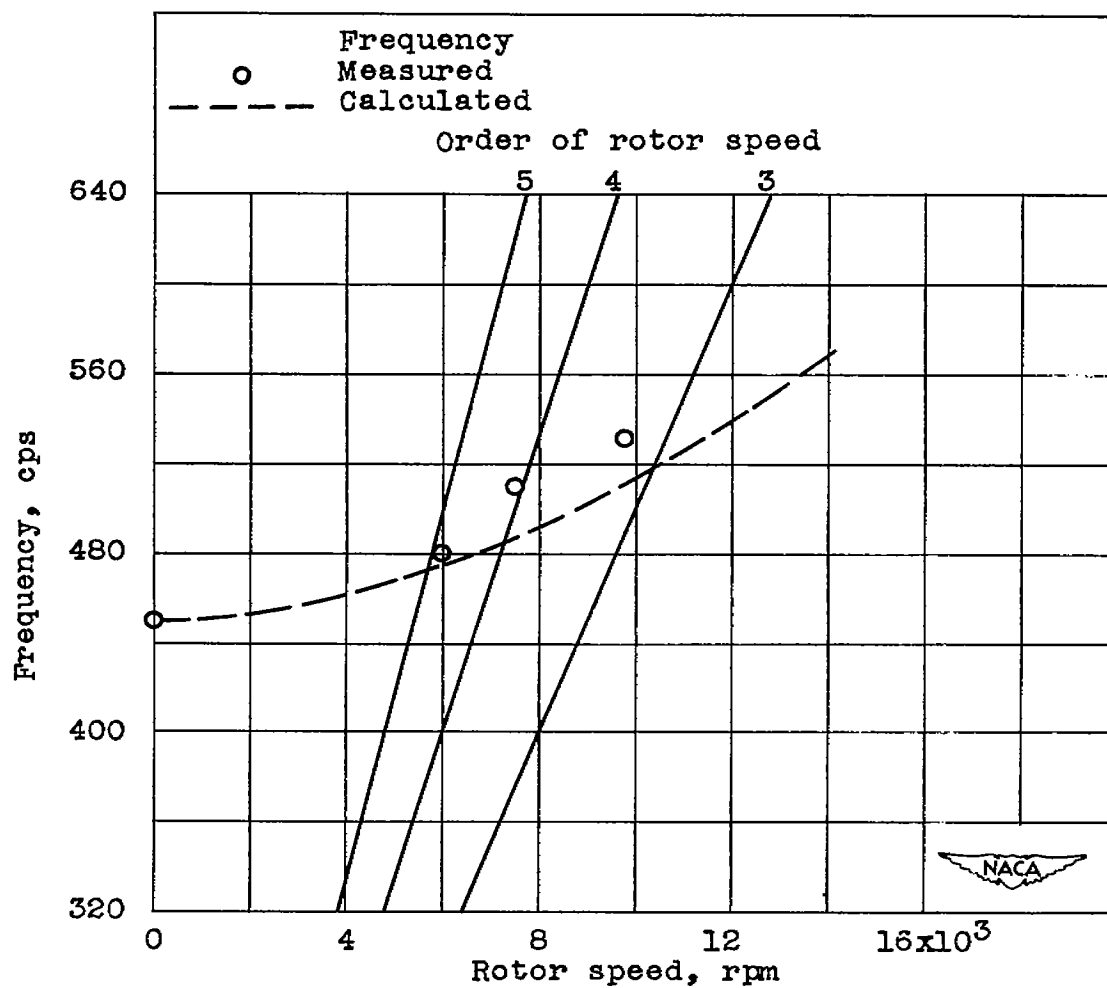
(a) First stage.

Figure 3. - Critical-speed diagram showing measured and
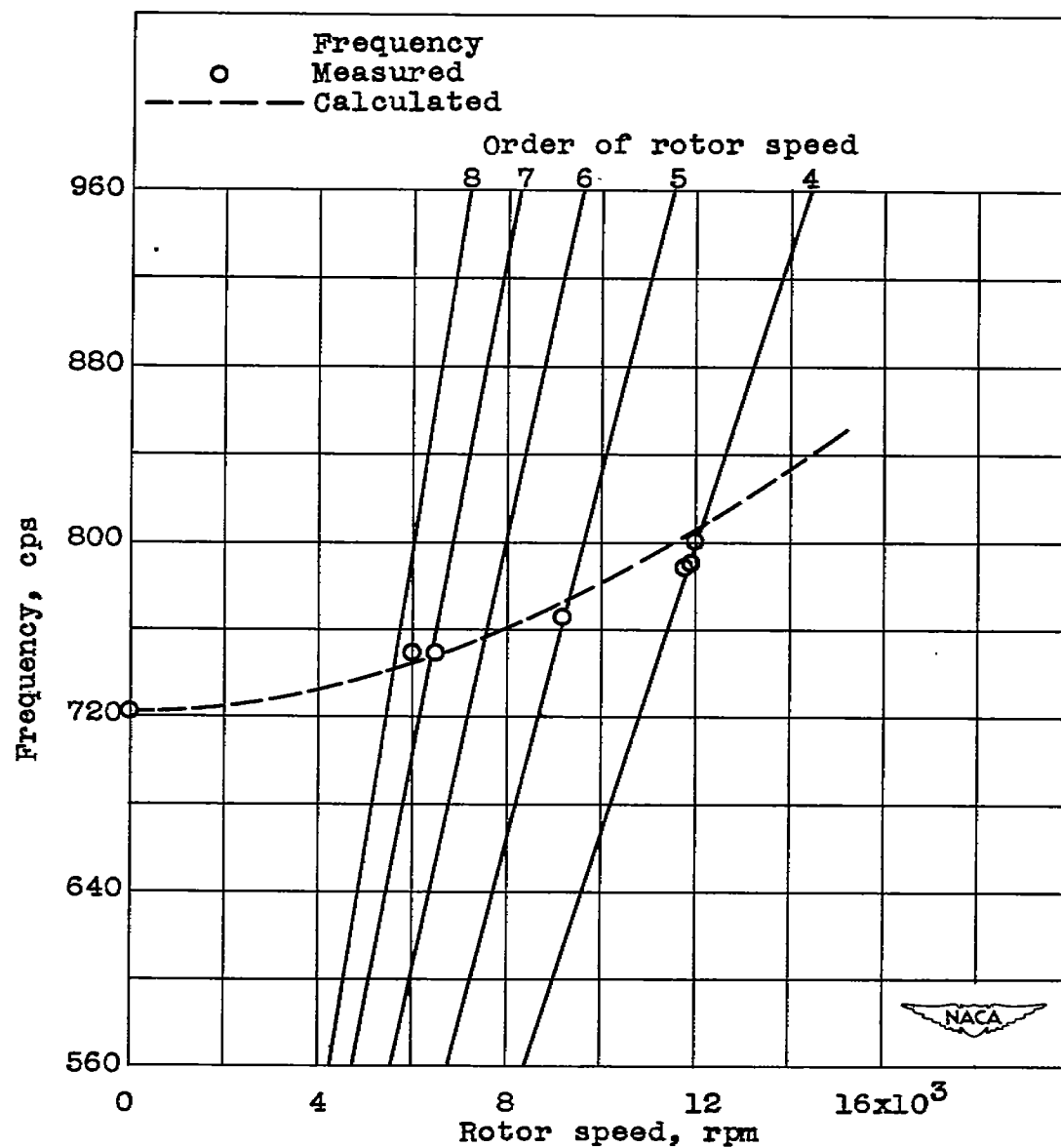calculated first bending-mode frequencies.
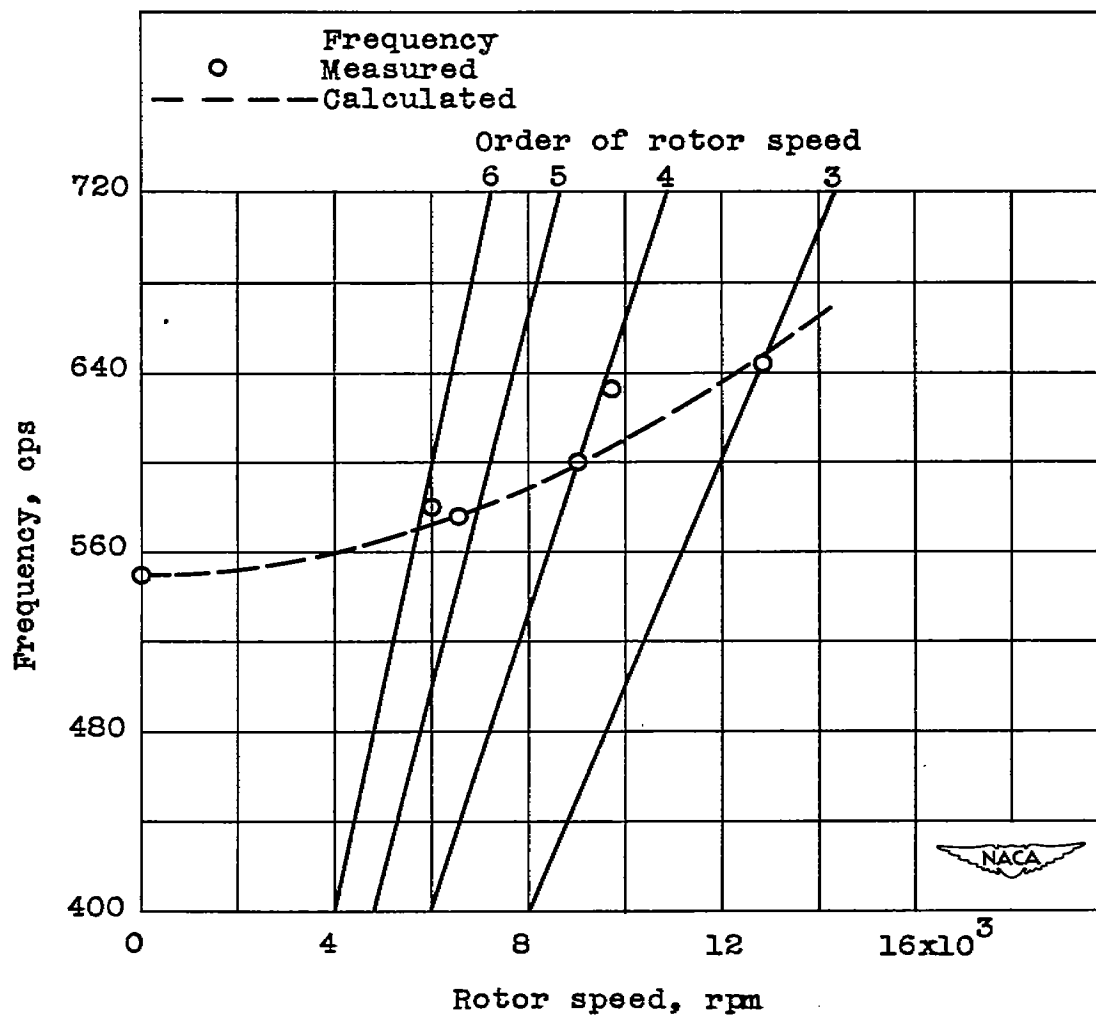
(b) Second stage.

Figure 3. - Continued. Critical-speed diagram showing
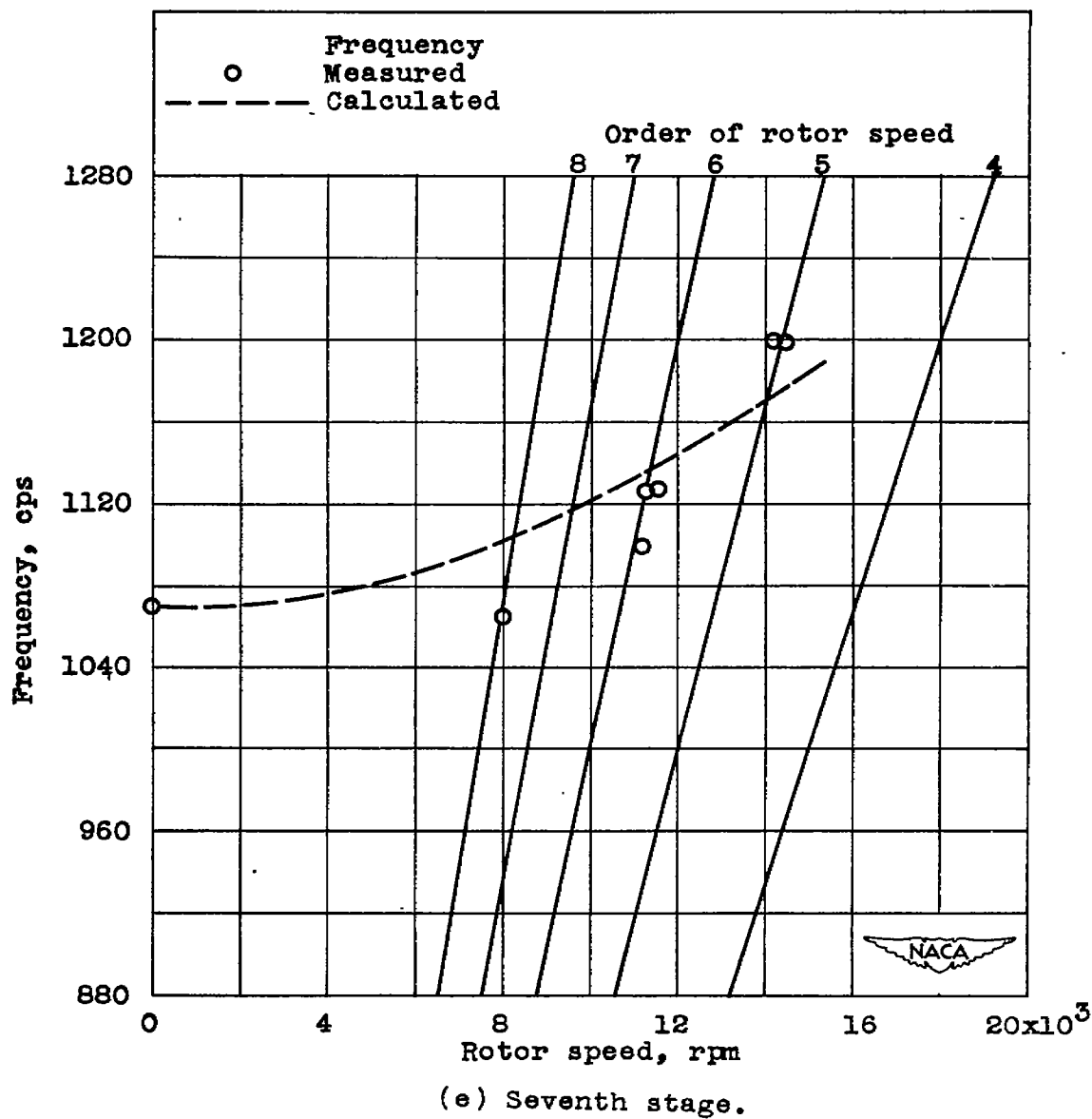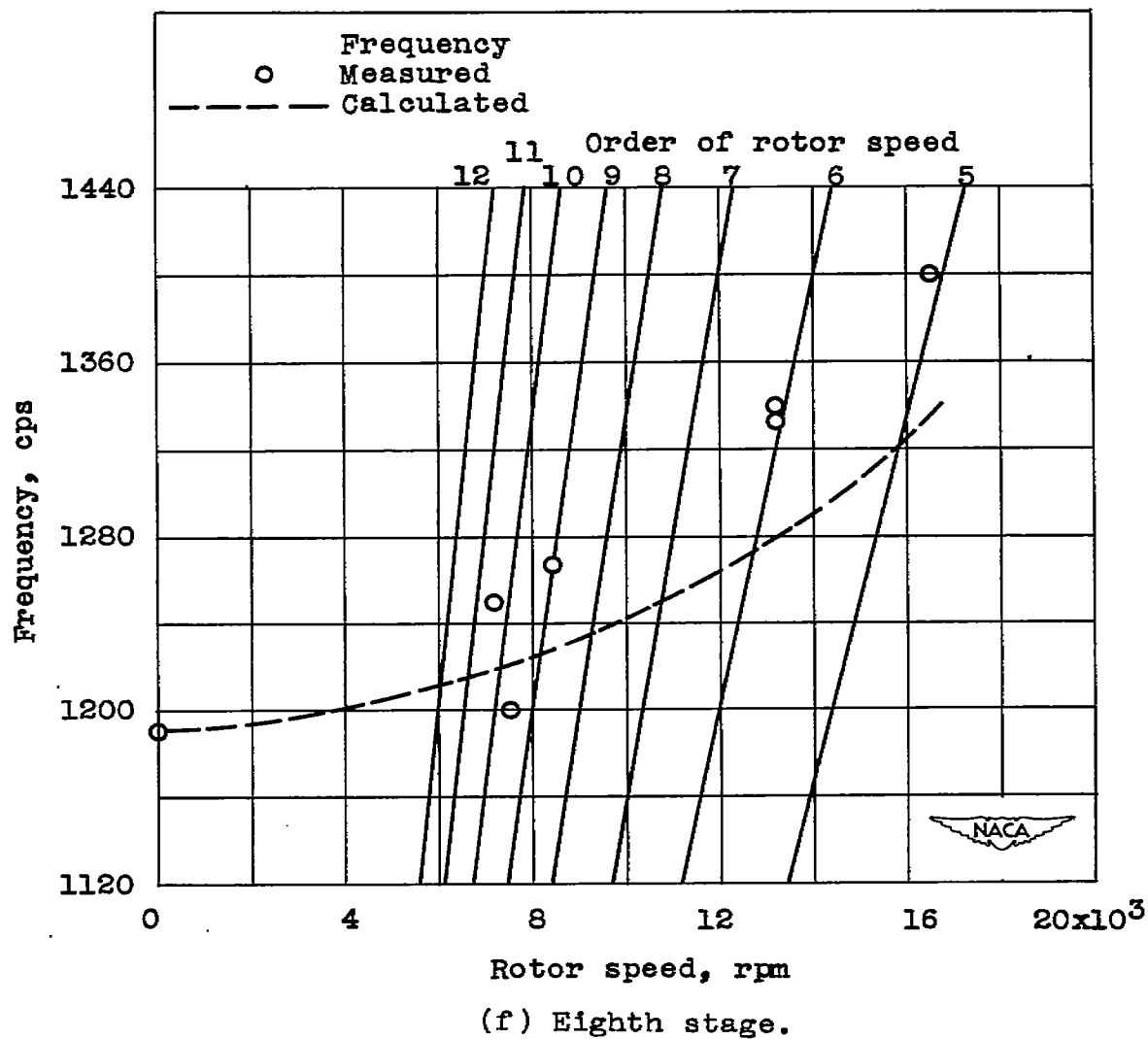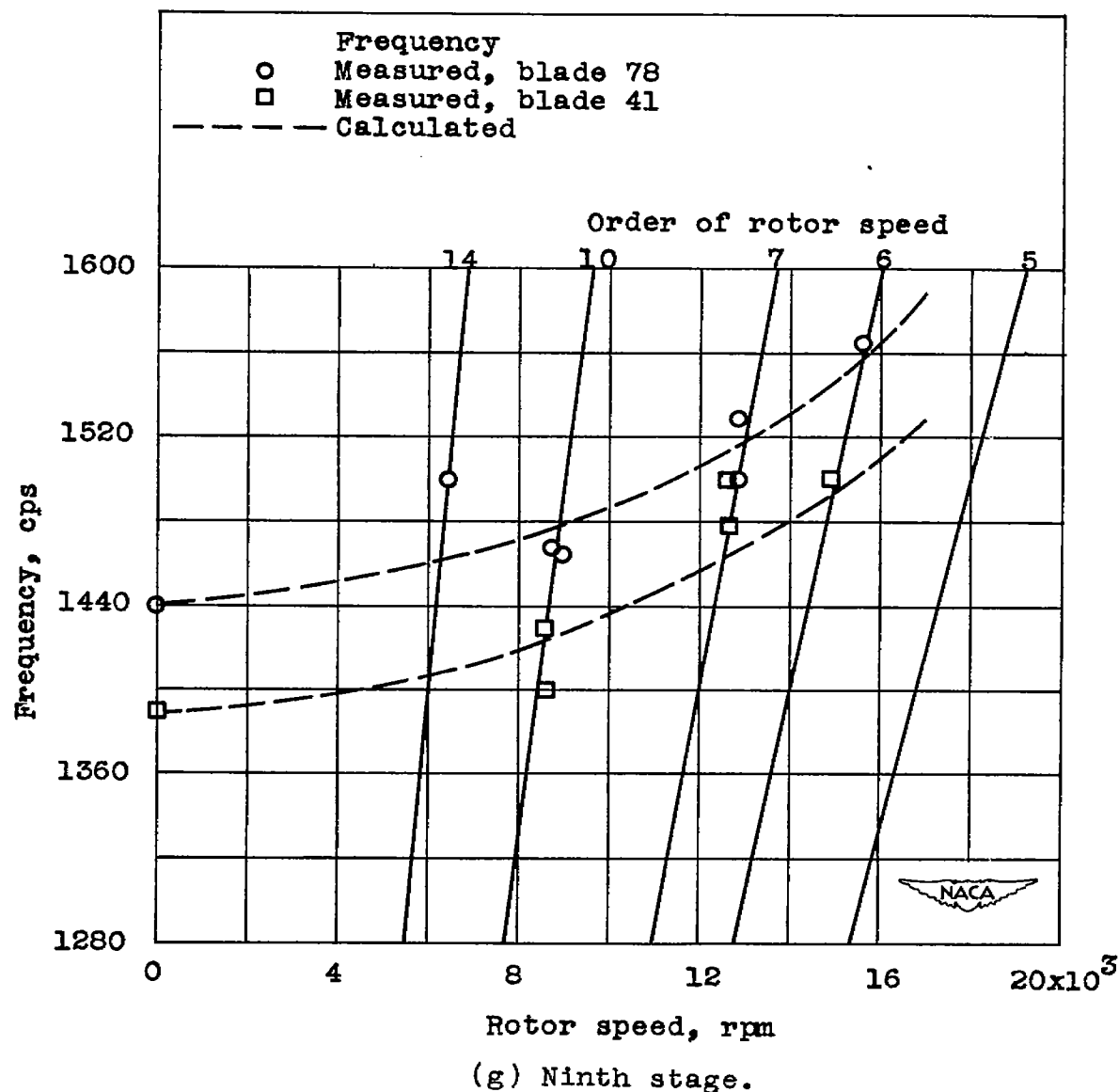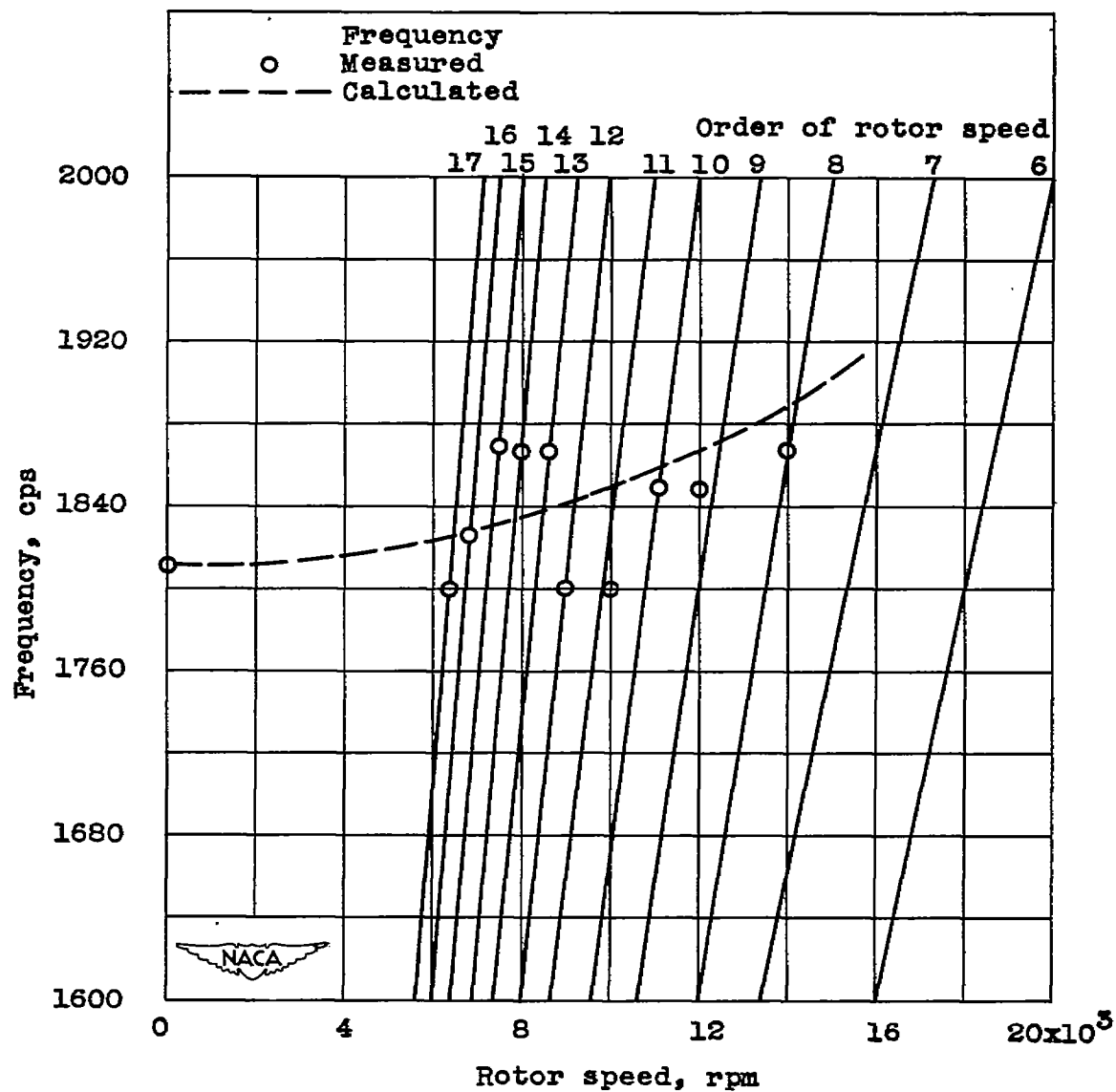measured and calculated first bending-mode frequencies.

(c) Third stage.

Figure 3. - Continued. Critical-speed diagram showing measured and calculated first bending-mode frequencies.

906

(d) Fourth stage.

Figure 3. - Continued. Critical-speed diagram showing
measured and calculated first bending-mode frequencies.

(e) Seventh stage.

Figure 3. - Continued. Critical-speed diagram showing
 measured and calculated first bending-mode frequencies.

906

(f) Eighth stage.

Figure 3. - Continued. Critical-speed diagram showing
measured and calculated first bending-mode frequencies.

(g) Ninth stage.

Figure 3. - Continued. Critical-speed diagram showing
measured and calculated first bending-mode frequencies.

(h) Tenth stage.

Figure 3. - Concluded. Critical-speed diagram showing
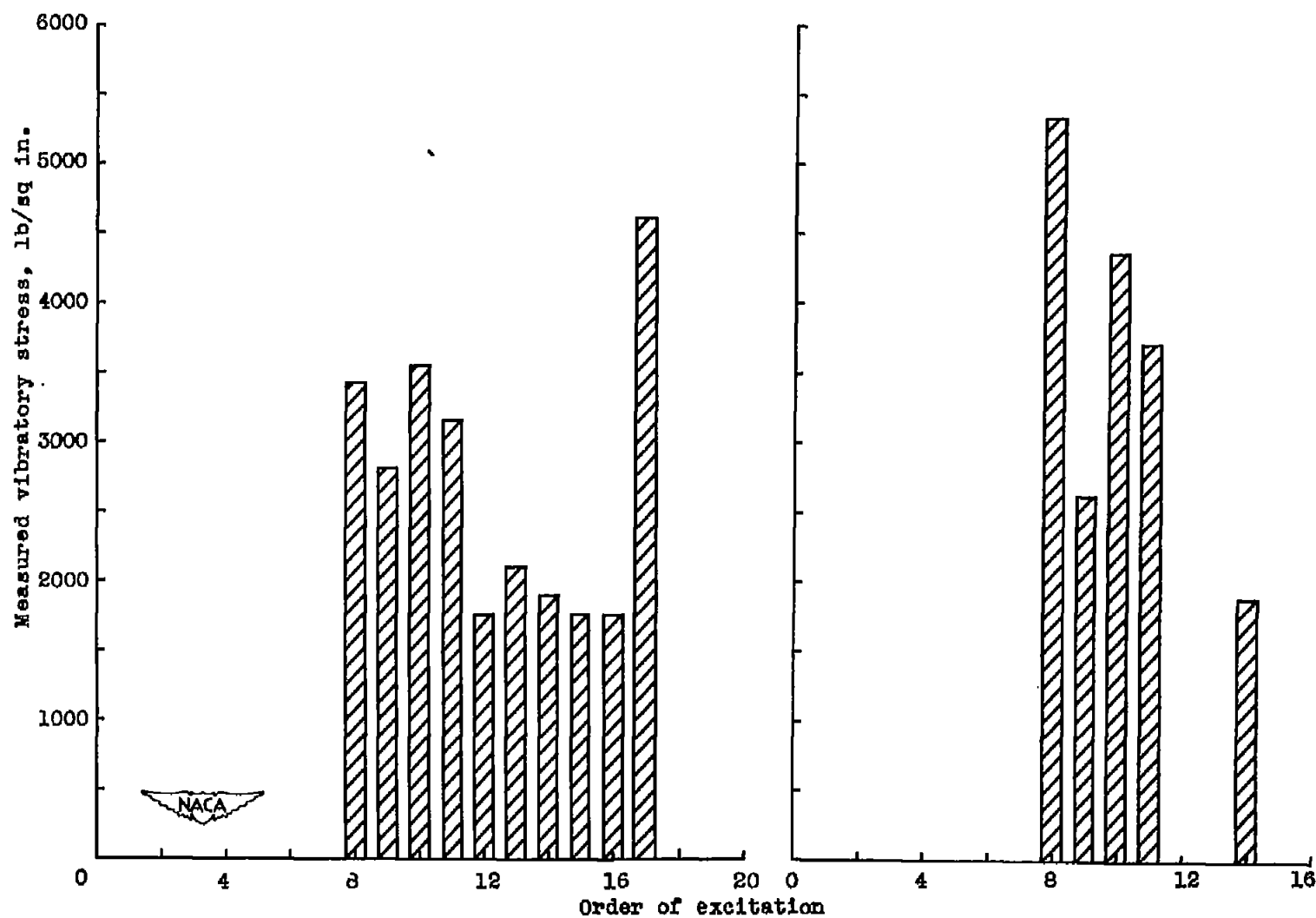measured and calculated first bending-mode frequencies.

(a) Seventh stage (blade 21).

(b) Eighth stage (blade 46).
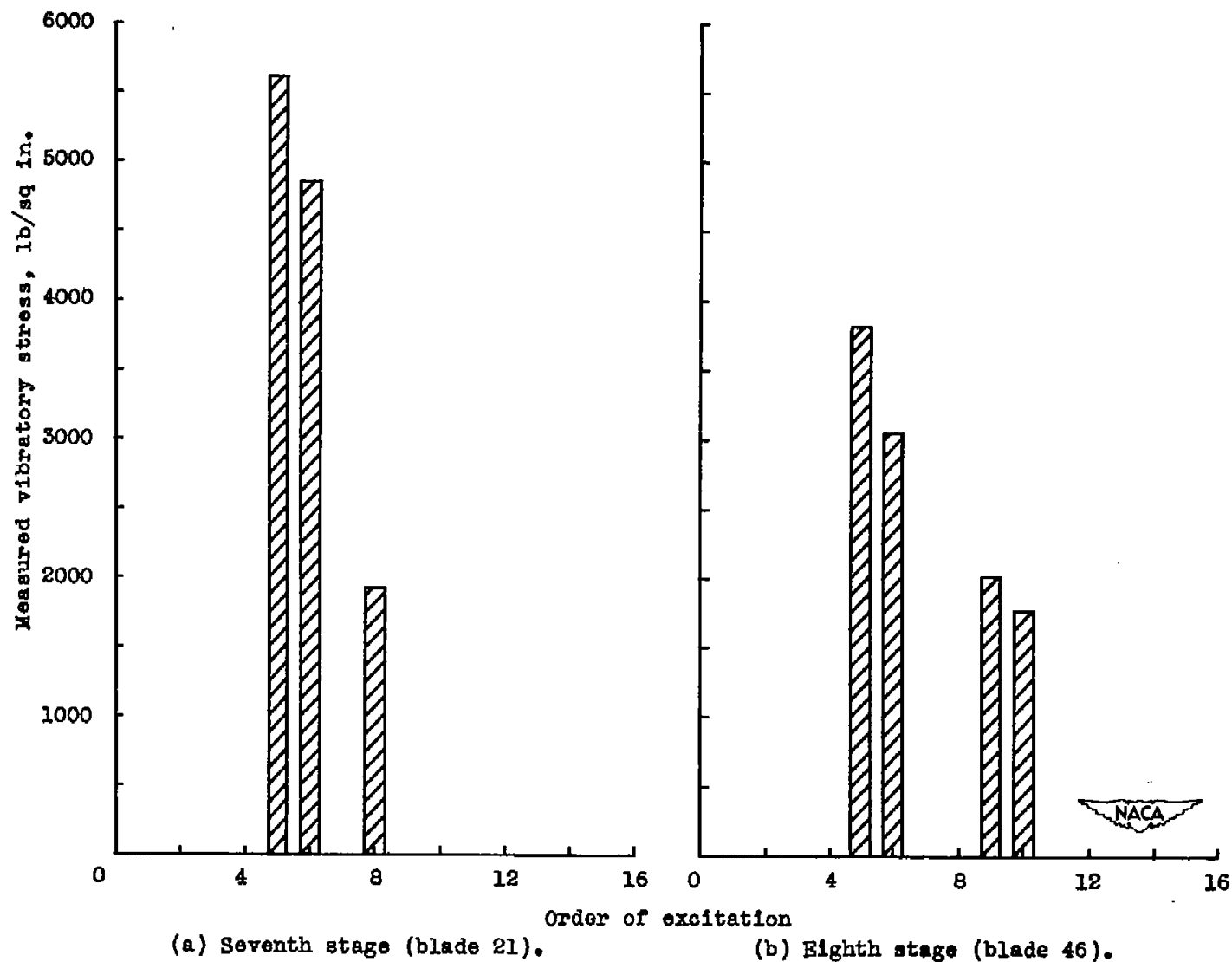
Figure 4. - Relation of magnitude of observed stresses to order of excitation.

(c) Tenth stage (blade 1).

(d) Tenth stage (blade 38).

Figure 4. - Concluded. Relation of magnitude of observed stresses to order number.
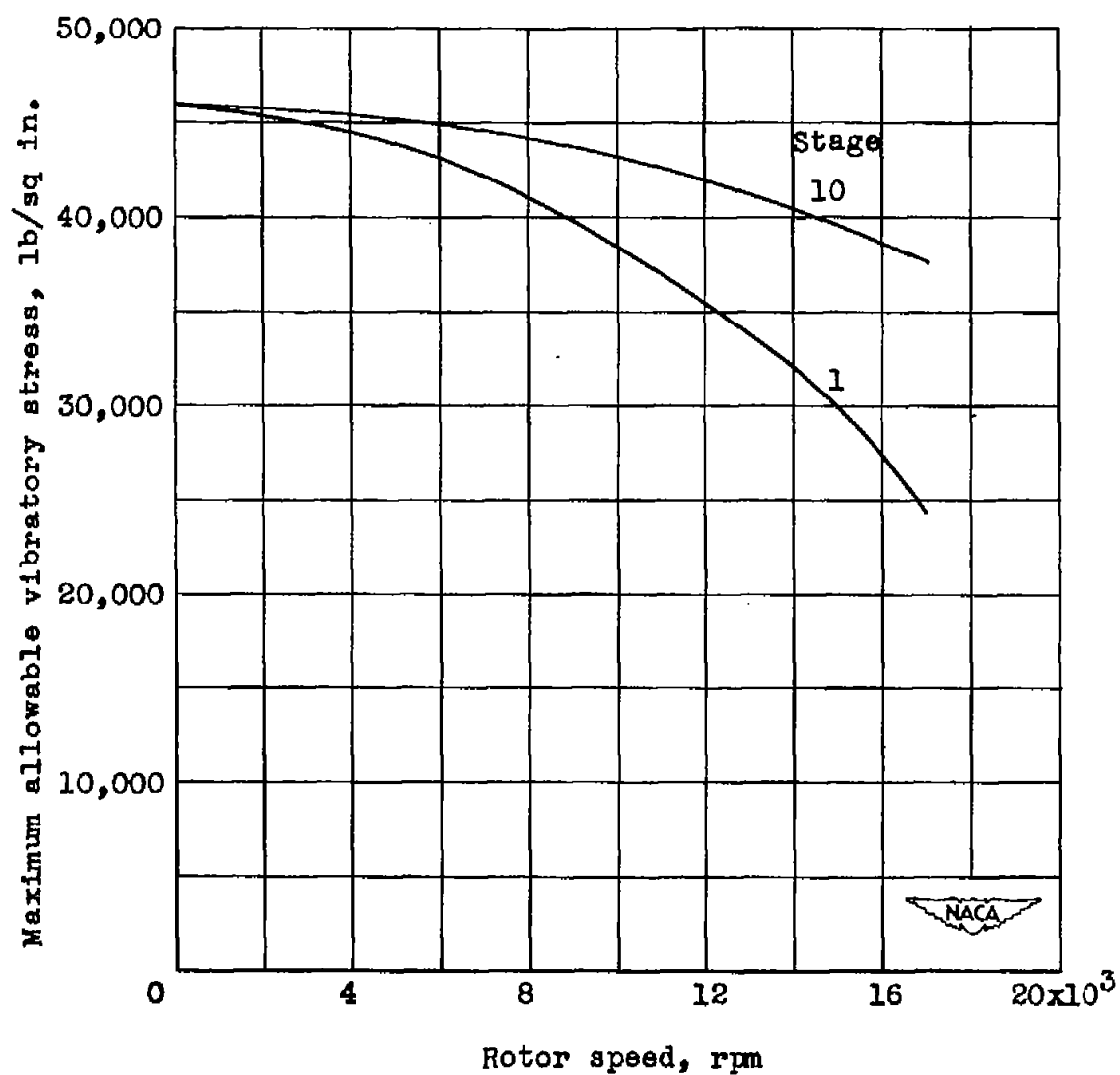
Figure 5. - Variation in maximum allowable vibratory stress
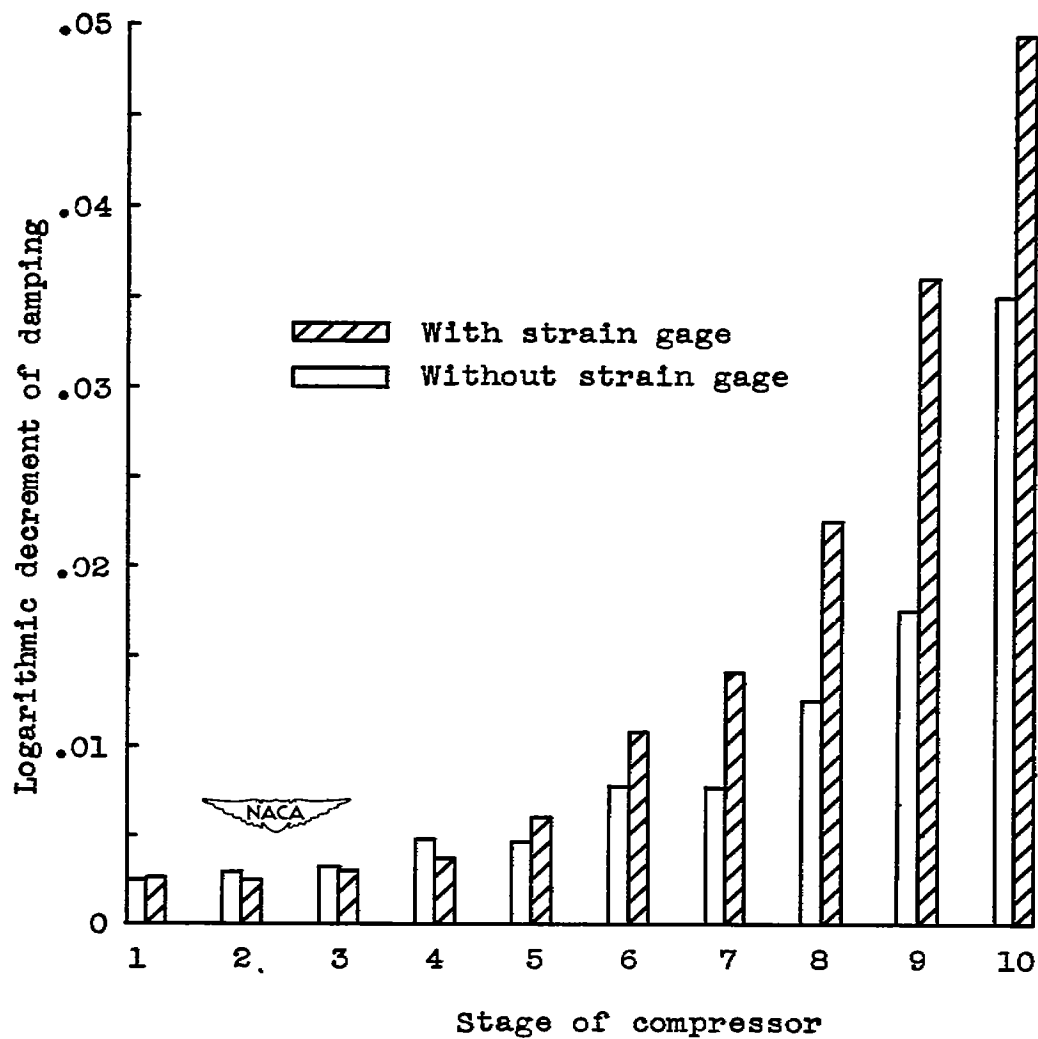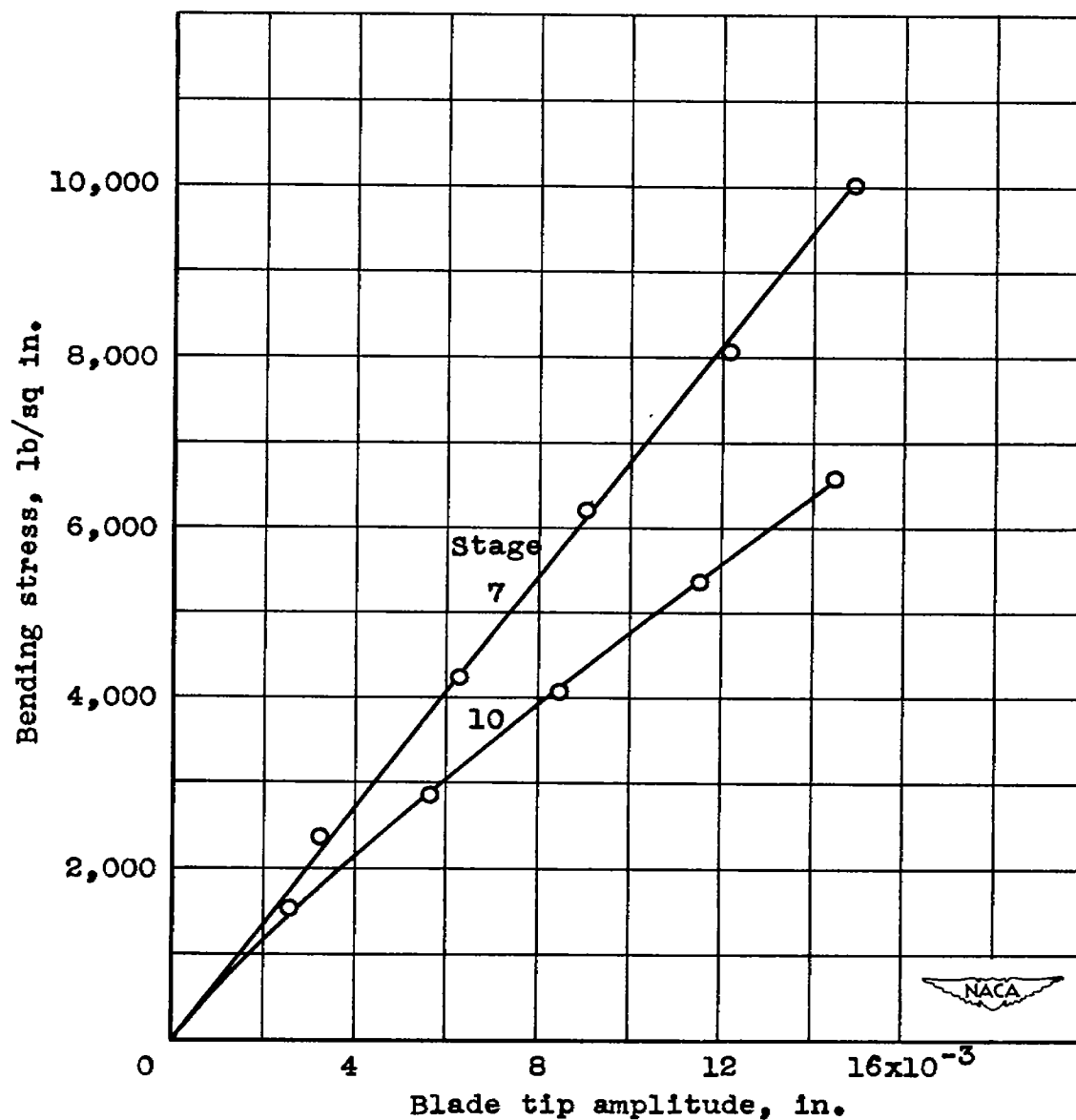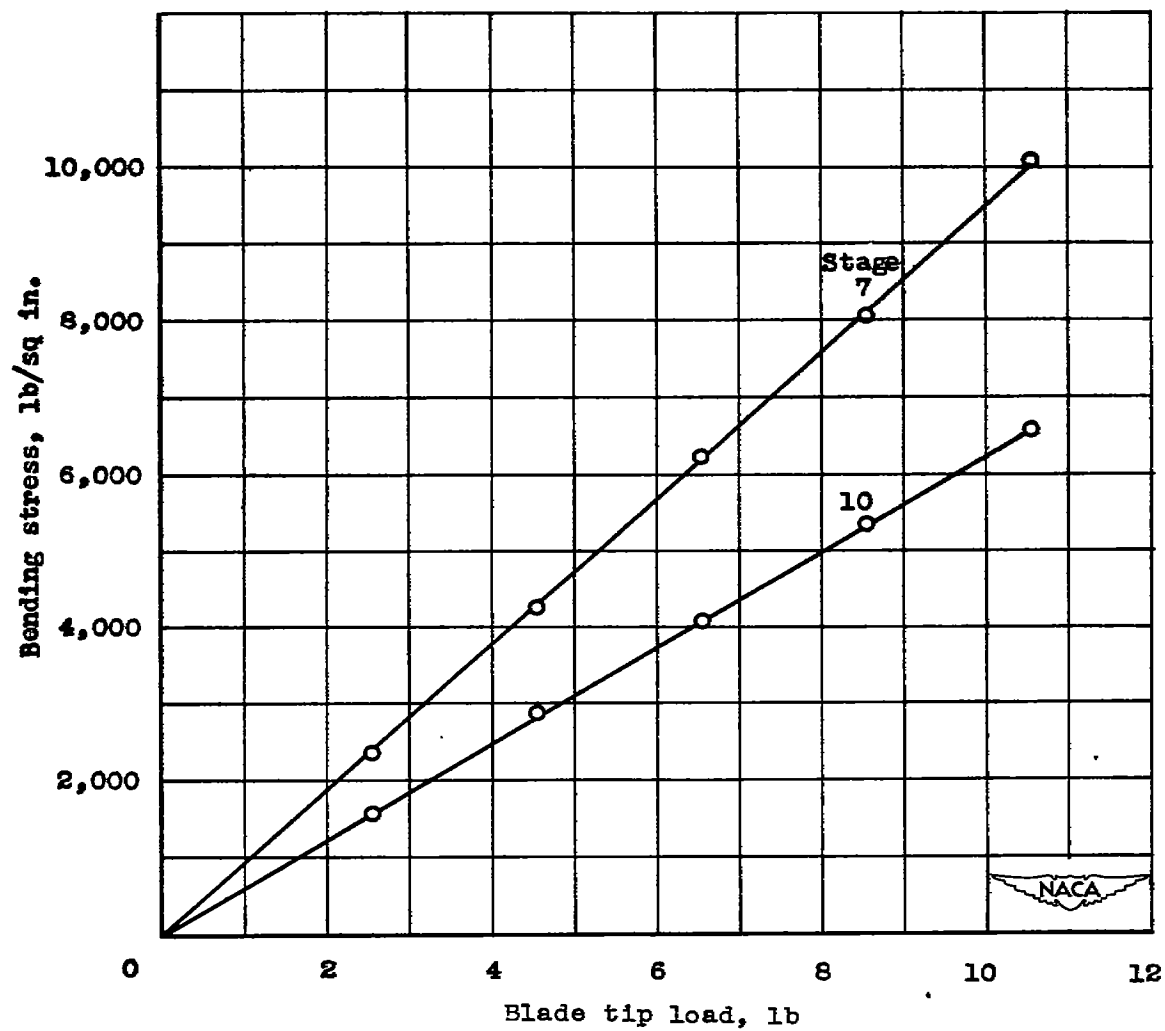with change in rotor speed.

Figure 6. - Damping of blades from all stages, with
and without strain gages.

(a) Tip amplitude.

Figure 7. - Static stress for blade tip amplitude and
loading.

(b) Tip loading.

Figure 7. - Concluded. Static stress for blade tip amplitude and loading.